

National Radio Astronomy Observatory  
**Electronics Division Technical Note No. 225**  
4-K Noise Measurements of LNF 4-16 GHz Amplifier with  
SAO Edge-Mode Isolator

Joseph Lambert

December 2, 2019

Contents

1	Introduction	2
2	Noise Temperature Measurement Setup	2
3	Baseline Measurements of the Amplifier Alone	3
3.1	DC Wiring Series Resistance Compensation . . . . .	4
3.2	Amplifier Settling Time . . . . .	4
4	Noise Measurements with Isolator	6
5	Summary	9
	References	10
	Appendices	11
A	Supplemental results using amplifier LNF-LNC4_16NRAOA s/n 010Z: Bias dependence and settling time	11

# 1 Introduction

SIS heterodyne receivers notoriously have a poor match between the mixer output and the IF preamplifier input. The DC conductance of the pumped mixer at its operating point may be close to zero, and can sometimes be negative due to the quantum mechanical nature of SIS mixers. The mismatch can lead to undesirable ripple in the IF passband, and some amplifiers can become unstable and oscillate in or outside the IF band. These issues have appeared in mixer-preamps where the mixer body is bolted directly to the IF amplifier in order to minimize loss, as in the current ALMA Band 6 receivers [1]. Introducing an isolator between the mixer output and amplifier input can help mitigate problematic mixer-preamp interactions. The main drawback with the inclusion of an isolator is significant increase in the receiver noise temperature due to the added loss of the isolator right at the point of lowest signal-to-noise in the receiver. Additionally, a primary goal of the ALMA Band 6 upgrade is an increase of the IF bandwidth, which presents the added challenge of developing a low-loss *and* wideband isolator compatible for cryogenic operation.

The Smithsonian Astrophysical Observatory (SAO) developed a promising edge-mode isolator with a frequency range of 4-20 GHz [2] for the wideband upgrade of the Sub-millimeter Array (wSMA). The design specifications were for insertion loss not to exceed 0.7 dB from 4-12 GHz and 1.0 dB from 12-20 GHz with good isolation and port match. These specifications should also be sufficient for the ALMA Band 6 upgrade. The cryogenic S-parameters were measured and reported in Ref [3]. In this note, we report on noise temperature measurements of the isolator. Specifically we quantify the effect of the isolator on the IF contribution to the receiver noise temperature. The method outlined here compares the measured noise temperature of the combined isolator and amplifier assembly, versus the amplifier alone.

# 2 Noise Temperature Measurement Setup

The cryogenic noise measurement setup uses the Y-factor method with a noise diode at the Dewar input, and spectrum analyzer at the output. The signals to and from the amplifier are carried by three sections of UT-085 coaxial cables: two sections of lossy stainless steel UT-085-SS-SS cables from room temperature to the radiation shield ( $\sim 30$  K), and from the radiation shield to the cold plate ( $\sim 3.5$  K), followed by low loss UT-085-TP<sup>1</sup> coaxial cables connected from the cold plate to the device under test. A 20 dB cold attenuator is connected at the amplifier input to reduce the effective ENR, the define the cold load temperature seen by the amplifier, and to reduce uncertainties in the noise contributions of the preceding cables.<sup>2</sup> The full schematic of the measurement system is shown in figure 1. The loss and effective noise temperatures of the cables and attenuator were carefully characterized and calibrated. Software written in Python was developed to collect the data from the spectrum analyzer, perform the corrections for the loss/gain and noise contributions of all components

---

<sup>1</sup>Silver plated copper-weld center conductor, tin-plated copper outer conductor, PTFE dielectric.

<sup>2</sup>The cables with endpoints at different temperatures have a nonlinear temperature and loss gradient along their length, which are difficult to model accurately. The noise contribution of a cable is approximated as a discrete element with loss equal to the total measured loss of the cable in situ while the system was cold, and physical temperature equal to the arithmetic mean of the endpoint temperatures.

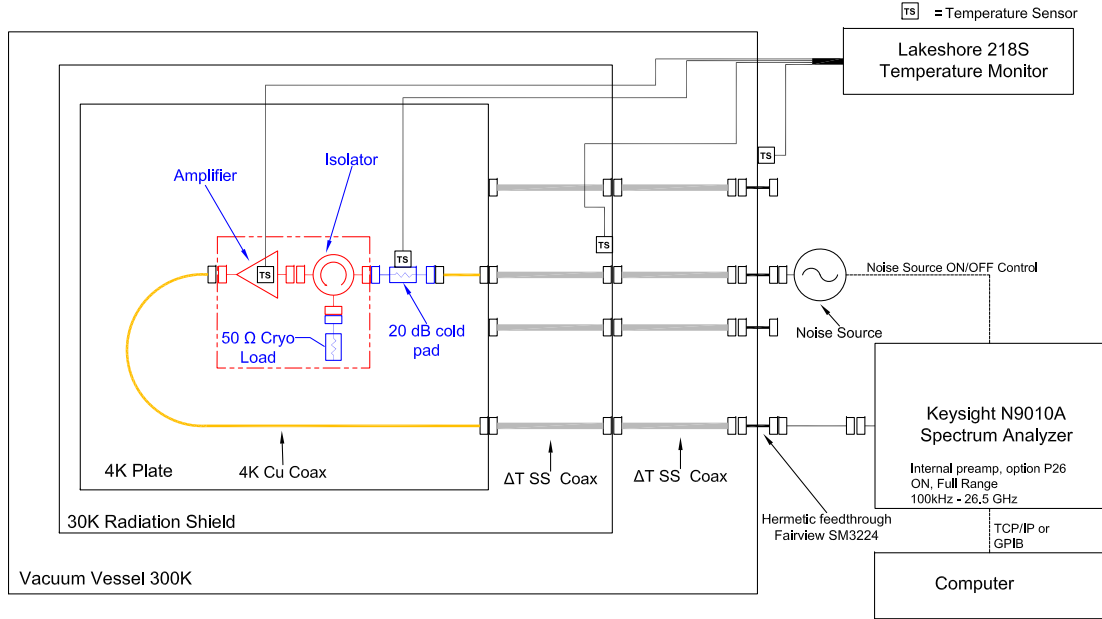


Figure 1: Schematic of the cryogenic noise temperature measurement system. The dashed box in red outlines the assembly under test.

and instruments of the test system, perform the Y-factor calculations, and record and plot the data.

### 3 Baseline Measurements of the Amplifier Alone

The amplifiers used are from Low Noise Factory, model LNF-LNC4\_16B, serial numbers 1654Z and 1537Z, which operate over 4-16 GHz. The two amplifiers performed very similarly, so we primarily focus on results from s/n 1654Z. The amplifiers alone were first carefully characterized for repeatability, and gain and noise stability. These characterizations are important because the measurements herein of the isolator assume the amplifier gain and noise temperature are constant over time and repeatable between cool down cycles. The noise characterization of the isolator requires, at minimum, two separate cool downs.

From previous measurements of LNF amplifiers, of models different from the ones used in the present measurements, it was found that the amplifiers were sensitive to the DC biasing conditions in two respects: first, it was important to correct the drain voltage as measured at the bias supply to compensate for the voltage drop across the resistive phosphor

bronze (PhBr) wires in the test Dewar. Second, it was found that the amplifier gain, noise temperature, and the settling time were sensitive to the DC biasing state and history (see appendix A for clear examples of these issues).

### 3.1 DC Wiring Series Resistance Compensation

The PhBr wire used to supply the drain current adds an additional  $R_{PhBr} = 16 \Omega$  resistance in series with the amplifier bias circuit, where  $R_{PhBr}$  is the total series resistance of the drain and ground wires. Although the resistivity of phosphor bronze wire is weakly dependent on physical temperature compared to e.g. copper, the resistance of the wiring was measured in situ with the system cold.<sup>3</sup> The drain voltage measured at the bias supply includes an additional voltage drop equal to  $V_{PhBr} = R_{PhBr} \cdot I_d$ . This additional voltage drop can be particularly significant for LNF amplifiers because drain currents are often up to 20 mA for optimum cryogenic operation. To accommodate the additional voltage drop, the total drain voltage at the bias supply should be:

$$V_{d,supply} = V_{d,amp} + R_{PhBr} \cdot I_d. \quad (1)$$

The amplifier alone was measured during a single cool down at three bias points, as shown in figure 2. The red curves are with no correction for the bias wire resistance, the blue curves are with the correction, and the green curves are for another arbitrary bias point to further illustrate the bias dependence. The black dashed lines are the measurements of the amplifier from the Low Noise Factory datasheet [4]. One can see that with the bias voltage correction, the gain curve matches the LNF data more closely. The noise temperature does not seem to be strongly affected by the DC bias voltage for this amplifier, however, other LNF models have shown a stronger bias voltage dependence on the noise temperature. See for example figures 7-9 in appendix A.

### 3.2 Amplifier Settling Time

For some LNF amplifiers measured previously, it was found that the time required for the amplifier gain and noise temperature to settle to constant values depended on the bias point and biasing history. A full investigation into the effects of biasing history is beyond the scope of this report. Instead, a consistent biasing procedure was adopted to ensure a reasonably repeatable result. The biasing procedure was as follows:

---

<sup>3</sup>The in situ resistance of the wires while cold was measured by shorting together the drain and ground wires at the cold end, and measuring the series resistance of the two wires.

Amp: LNF-LNC4\_16B sn 1654Z

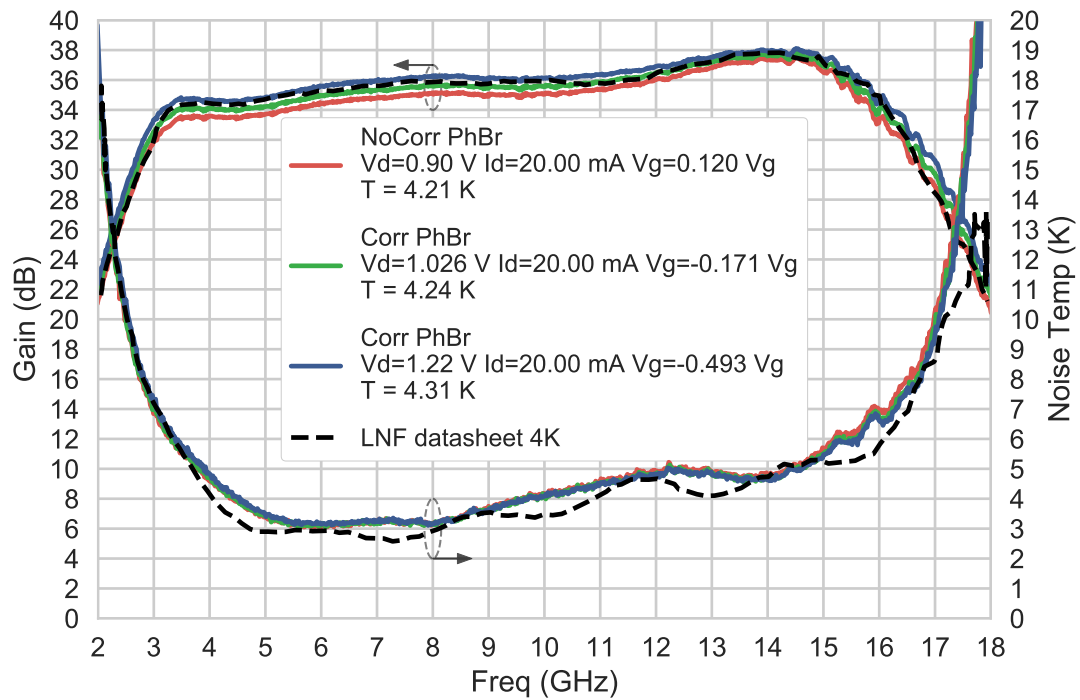


Figure 2: The cryogenic noise temperature and gain of the LNF amplifier alone, model LNF-LNC4\_16B, s/n 1654Z. Measured at three bias points with voltages and currents indicated in the legend as measured at the amplifier bias supply. The red curves use the nominal bias values as given in the datasheet from LNF. The blue curves use bias values that compensate for the series resistance of the bias wires, as described in the text. The green curves use another arbitrary bias point to further illustrate the bias dependence. The black dashed lines are the measurements provided in the LNF datasheet [4].

1. Preset the bias supply  $V_d$  and  $I_d$ , then turn off the bias supply and let the amplifier settle for at least 10 minutes.<sup>4</sup>
2. Turn on the bias supply and immediately start collecting a repeated series of measurements over time to monitor how and when the gain and noise temperature settles to constant values.
3. Repeat starting at step 1 for each change in bias parameters.

The present amplifiers used for the noise temperature evaluation of the wide-band edge-mode isolators were fortunately less susceptible to drift over time, as observed in the time-series data shown in figure 3. Two of the three bias points (red and blue) showed a very small, but noticeable, drift in the gate voltage over time. With corrected drain voltage (blue) the gate voltage seems to eventually settle to a constant value, whereas without correction (red) the gate voltage seems not to have reached a constant value at 30 mins. A third bias point (green) was found to be very steady, requiring almost no settling time. The noise temperature and gain appear to be very steady over the time period measured. The physical temperature increases with increasing DC power dissipation, as expected, but remains constant over the measured time period after an initial rise within the first few minutes.

A more pronounced DC bias dependence was observed for a different LNF amplifier, model LNF-LNC4\_16NRAOA, s/n 010Z, as presented in appendix A.

## 4 Noise Measurements with Isolator

A comparison of the amplifier alone and the amplifier with the SAO edge-mode isolator, s/n R6-17, is shown in figures 4 and 5 using two different amplifiers of the same model with the same isolator. The two figures together contain data from 4 separate cool down cycles. For each set of data, the biasing procedure described in section 3.2 was used, and the amplifier was allowed to settle for 30 minutes while biased at the prescribed values. The data show that at physical temperatures of  $\sim 4$  K over the frequency range of 4 to 16 GHz, the isolator contributes on average about 1 K to the noise temperature, with a maximum and minimum contribution of  $\sim 2$  K and  $\sim 0.2$  K, respectively. As mentioned previously, the two amplifiers showed remarkably similar performance, and likewise the results with the isolator were very similar for the two amplifiers.

As a consistency check, the loss of the isolator can be inferred from the measured noise temperatures and compared to the directly measured insertion loss from S-parameter measurements. The inferred loss (or gain) is calculated as follows. The effective noise temperature of the isolator referred to its input is

$$T_e^{Iso} = T_{Phys}^{Iso} \left( \frac{1}{G^{Iso}} - 1 \right), \quad (2)$$

---

<sup>4</sup>Ideally, the bias to the amplifier should be toggled off and on by grounding/un-grounding the source leads. This would eliminate issues related to bias supply warm-up time and transients from the sudden power on of the bias supply. The method used, however, is sufficient for repeatability.

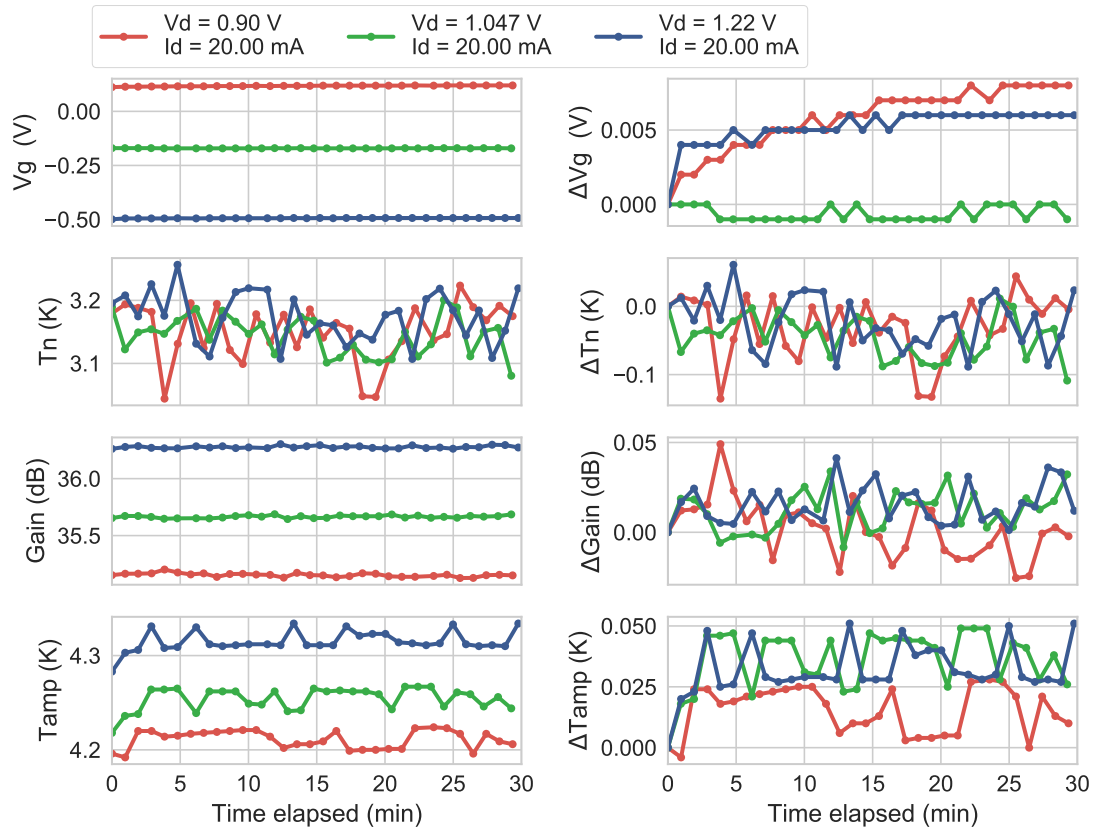


Figure 3: The evolution over time of the gate voltage, noise temperature, gain, and amplifier body physical temperature for the same three bias points plotted in figure 2 for amplifier LNF-LNC4\_16B, s/n 1654Z. The gain and noise temperature are plotted for a frequency of 8 GHz. The axes in the left column plot the measured values. The axes in the right column plot the difference from the initial value to more clearly show how the values change over time.

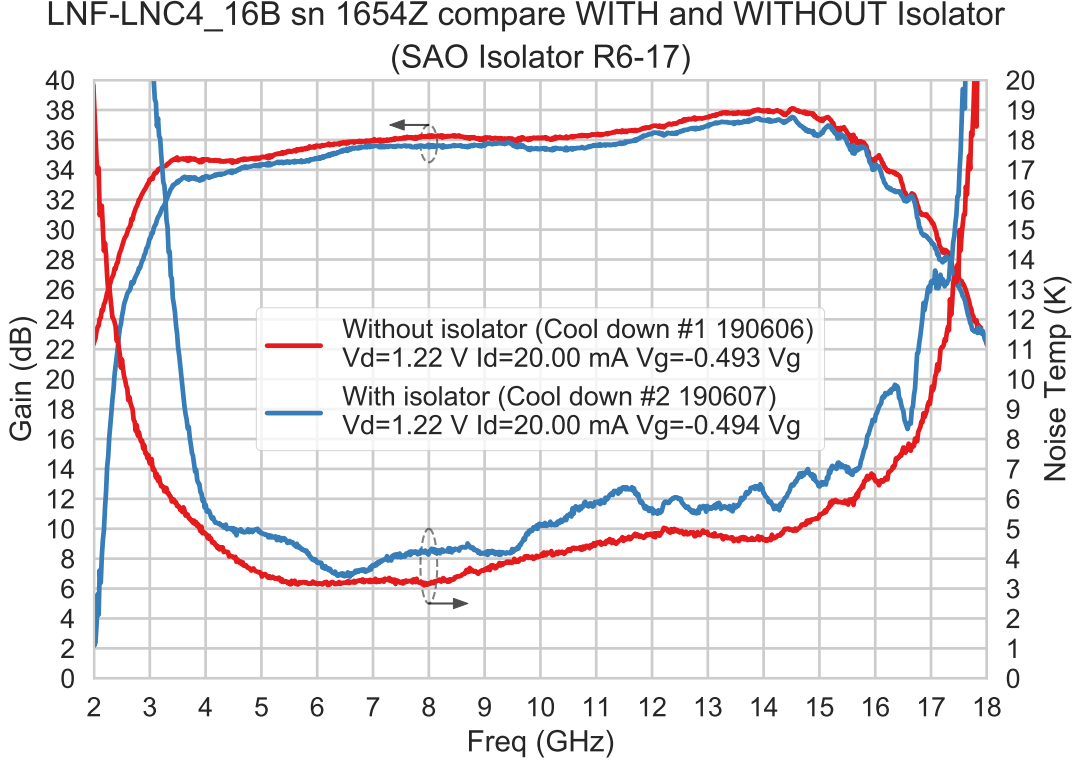


Figure 4: Comparison of the noise temperature and gain of amplifier LNF-LNC4.16B, s/n 1654Z, with and without the SAO isolator (s/n R6-17) at the amplifier input. DC bias with correction for the resistance of the system wiring was used, and the legend reports bias values as measured at the bias supply.

where  $T_{Phys}^{Iso}$  is the physical temperature of the isolator, and  $G^{Iso}$  is the gain of the isolator. The directly measured values are the effective noise temperature of the amplifier alone,  $T_e^{Amp}$ , and the effective noise temperature of the cascade of isolator and amplifier,  $T_e^{Cas}$ , referred to their inputs. The cascaded components are represented in the red dashed box in figure 1. The effective cascade noise temperature is expected to be:

$$T_e^{Cas} = \frac{T_e^{Amp}}{G^{Iso}} + T_e^{Iso}. \quad (3)$$

From equations 2 and 3, the inferred gain of the isolator is,

$$G^{Iso} = \frac{T_e^{Amp} + T_{Phys}^{Iso}}{T_e^{Cas} + T_{Phys}^{Iso}}. \quad (4)$$

These expressions do not explicitly take into account the effects of reflections, so the calculated isolator gain in equation 4 captures the effects of both the isolator transmission loss, and all additional reflection losses and their interferences.

The SAO edge-mode isolator loss is inferred from highest power dissipation bias points using amplifier s/n 1654Z, plotted in figure 6. The inferred gain of the isolator agrees



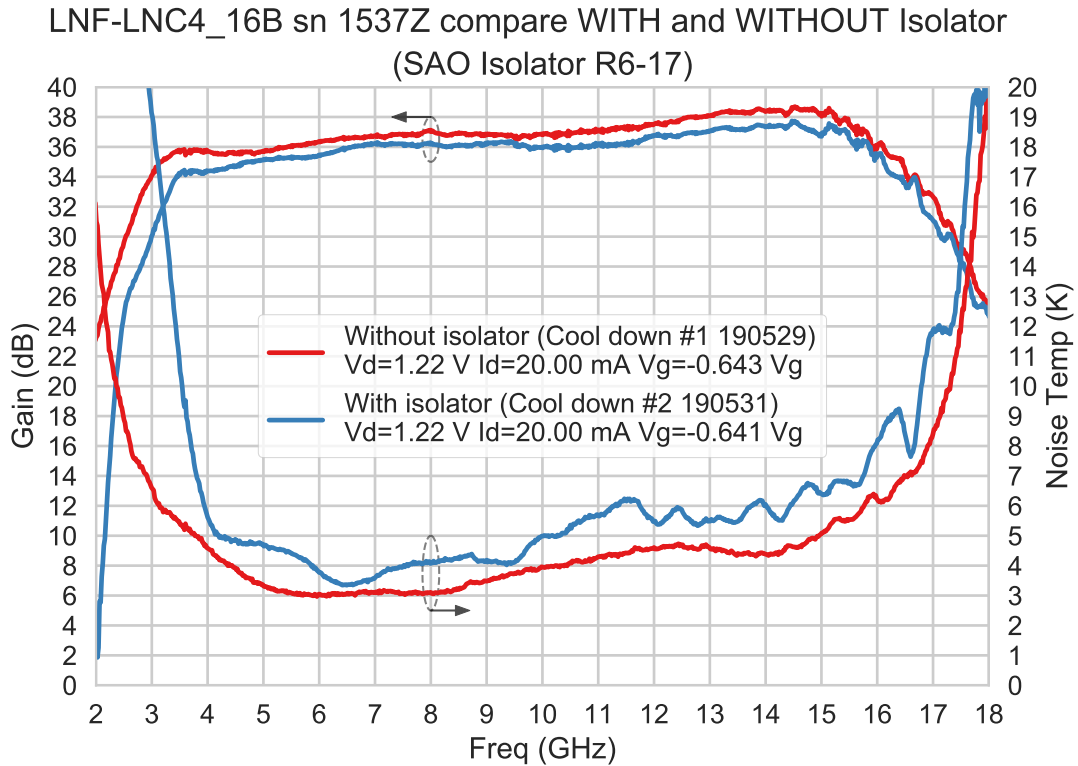


Figure 5: Comparison of the noise temperature and gain of amplifier LNF-LNC4.16B, s/n 1537Z, with and without the SAO isolator (s/n R6-17) at the amplifier input. DC bias with correction for the resistance of the system wiring was used, and the legend reports bias values as measured at the bias supply.

fairly well with the directly measured gain. There is significant ripple presumably due to impedance mismatches at the isolator ports, and between the amplifier input and the 20 dB cold attenuator. Similar results were obtained for other bias points and with LNF amplifier s/n 1537Z.

## 5 Summary

In summary, we have measured the noise contribution of a low-loss wideband edge-mode isolator when placed at the input of an IF preamplifier for use in SIS heterodyne receivers. The amplifiers were carefully characterized for repeatable and constant performance over time and between thermal cycles, so that comparison with and without the isolator can be made confidently. The inferred loss of the isolator from the noise temperature measurements generally matched the directly measured loss of the isolator from cryogenic S-parameter measurements. At physical temperatures around 4 K, it was found that the isolator contributed on average  $\sim 1$  K to the IF amplifier noise temperature over 4-16 GHz.

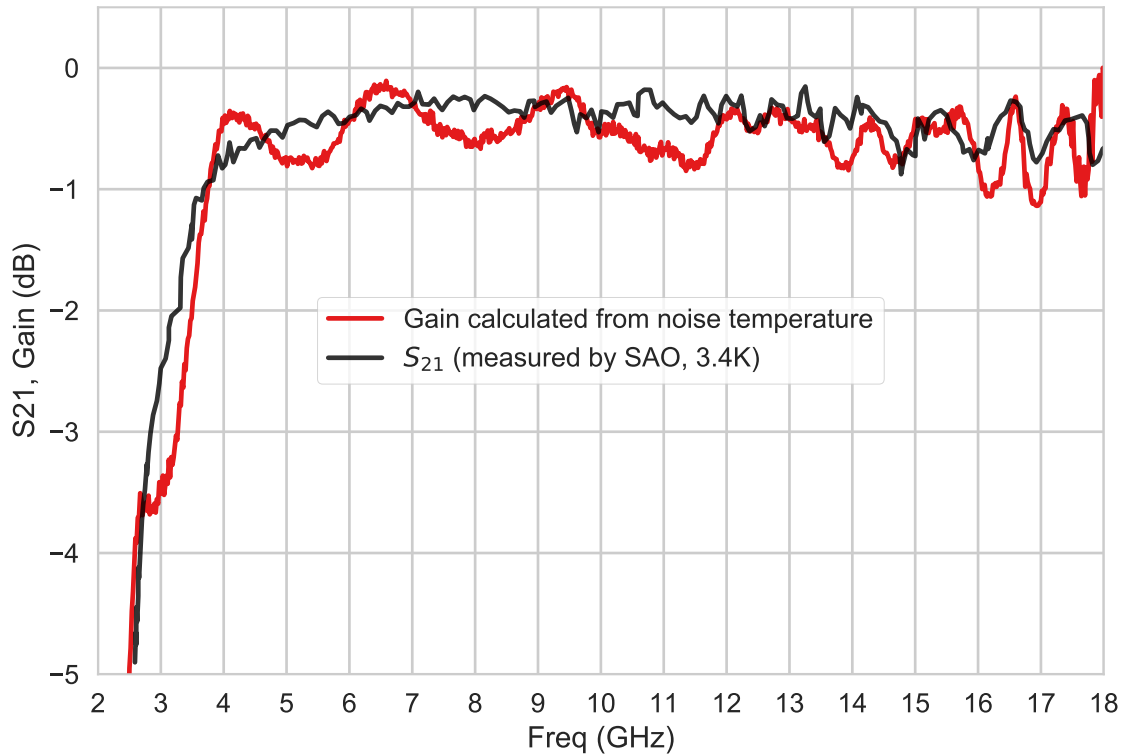


Figure 6: The inferred gain of the SAO isolator, s/n R6-17 (red) using the noise data in figure 4 with LNF amplifier s/n 1654Z, calculated using equation 4. The physical temperature of the isolator was 3.7 K. The black curve is the cryogenic  $S_{21}$  parameter measured by SAO, for comparison.

## References

- [1] A. R. Kerr, S.-K. Pan, S. M. X. Claude, P. Dindo, A. W. Lichtenberger, J. E. Effland, and E. F. Lauria, “Development of the ALMA Band-3 and Band-6 Sideband-Separating SIS Mixers,” *IEEE Transactions on Terahertz Science and Technology*, vol. 4, pp. 201–212, 1 2014.
- [2] L. Zeng, C. E. Tong, R. Blundell, P. K. Grimes, and S. N. Paine, “A Low-Loss Edge-Mode Isolator With Improved Bandwidth for Cryogenic Operation,” *IEEE Transactions on Microwave Theory and Techniques*, vol. 66, pp. 2154–2160, 2018.
- [3] P. Dindo, “S-Parameter Measurements of an SAO Edge-Mode Isolator at 4 K,” *Electronics Division Technical Note no. 224*, 2019. <http://library.nrao.edu/edtn.shtml>.
- [4] [https://www.lownoisefactory.com/datasheets/LNF-LNC4\\_16B\\_sn1654Z.pdf](https://www.lownoisefactory.com/datasheets/LNF-LNC4_16B_sn1654Z.pdf).

# Appendices

## A Supplemental results using amplifier LNF-LNC4\_16NRAOA s/n 010Z: Bias dependence and settling time

Here we show additional data to help illustrate the DC bias dependent behavior seen in some amplifiers. Extensive measurements of the SAO edge-mode isolator were first done with a similar model of LNF amplifier (model: LNF-LNC4\_16NRAOA) which has an NRAO bias chip integrated into the amplifier input for DC biasing SIS mixers. The presence of the bias chip lowers the upper frequency end from 16 to 13 GHz. These amplifiers showed more pronounced bias dependence in their gain and noise temperature as discussed in section 3.

In figures 7-9, we plot the gain and noise temperature for three power dissipation bias points, BP1, BP2, and BP3, respectively, both corrected and uncorrected for the resistance of the phosphor bronze bias wires. For all three power dissipations, it is clear that correction to the drain voltage is required to match the results from Low Noise Factory. Also, the discrepancies become more pronounced with the lower power dissipation.

Time series data is shown in figure 10. Here we see that the gate voltage, noise temperature and gain stay more constant over time for the higher power dissipation bias settings. At the lowest power dissipation, the amplifier appears never to cease drifting up to 30 mins after initially powering on the amplifier. Also, the amplifier performance is steadier when the bias wire resistance is accounted for, as seen for the solid lines. The amplifier drift is not attributed to the physical temperature of the amplifier as the physical temperature remains constant within measurement error for all bias settings

In figures 11-13, we show the comparison of gain and noise temperature with and without the isolator, for the three power dissipation levels. The measured noise contribution of the isolator with this amplifier is nearly identical to the measurements with the amplifier presented in the main text of this report. Of significance from these figures, the amplifier with the isolator was measured during two separate thermal cycles. The excellent repeatability of the amplifier performance is apparent in the highest power dissipation data, figure 11. As the power dissipation is lowered, the repeatability becomes progressively worse. These results motivated the use of the highest power dissipation, with correction for DC bias wire resistance, for determining the isolator contribution to the noise temperature.

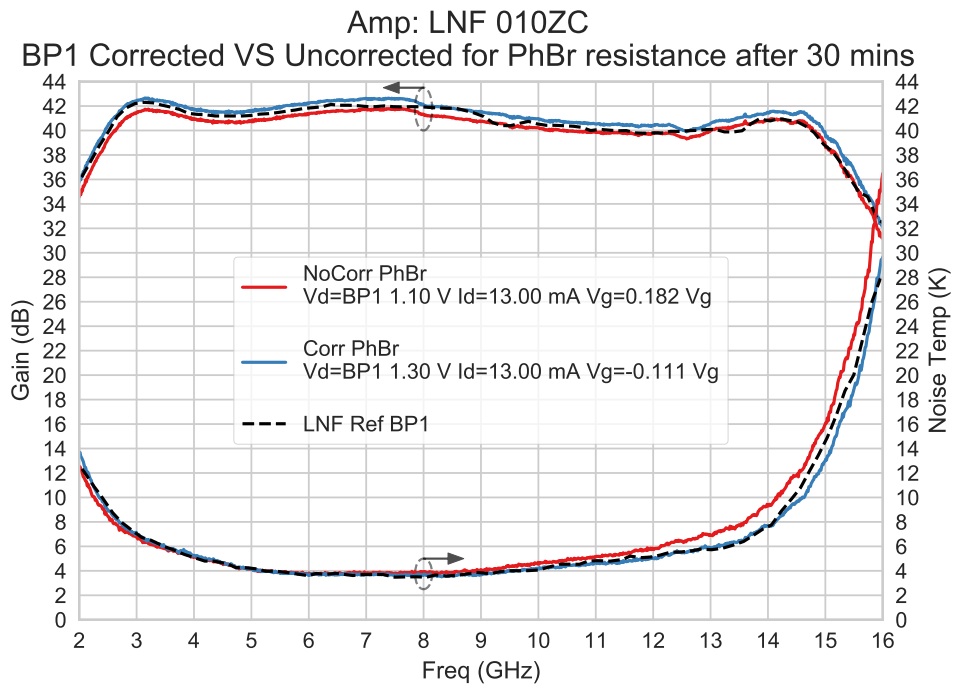


Figure 7: The gain and noise temperature of amplifier LNF-LNC4.16NRAOA s/n 010Z with (blue) and without (red) correction for the DC bias wire resistance, for the highest power dissipation bias. The black dashed lines are the measurements from the amplifier datasheet ([www.lownoiseefactory.com/datasheets/LNF-LNC4\\_16NRAOA\\_sn010Z.pdf](http://www.lownoiseefactory.com/datasheets/LNF-LNC4_16NRAOA_sn010Z.pdf)).

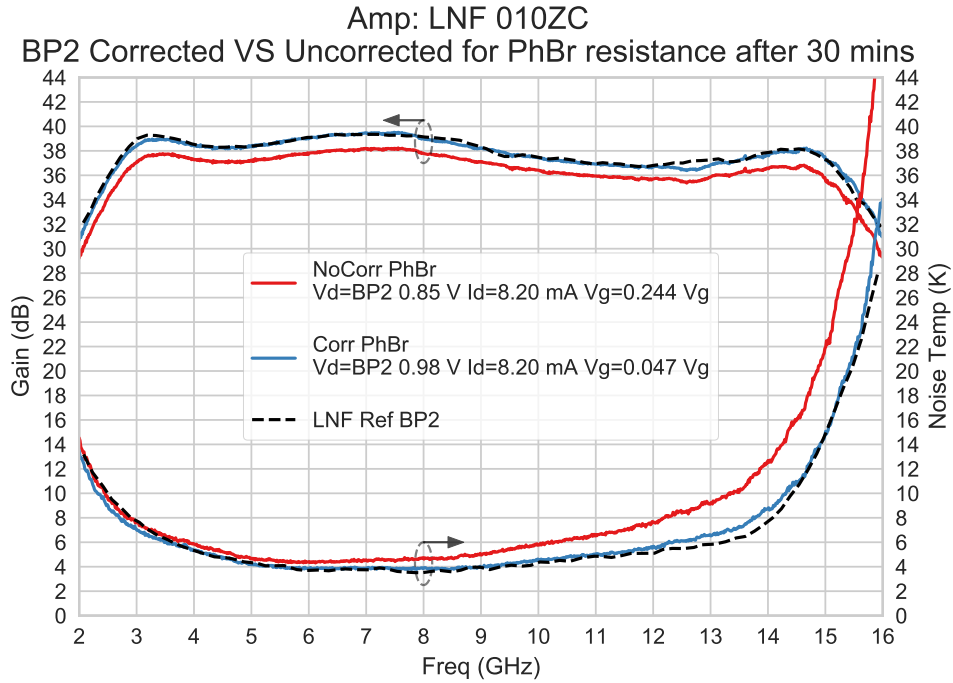


Figure 8: Similar to figure 7 for medium power dissipation bias.

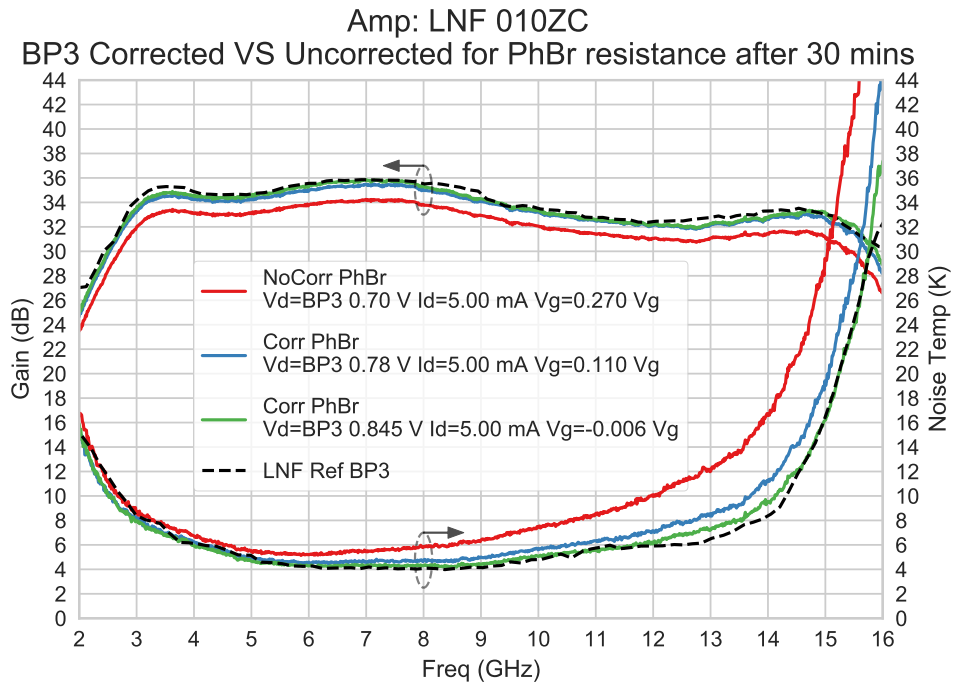


Figure 9: Similar to figure 7 for low power dissipation bias.

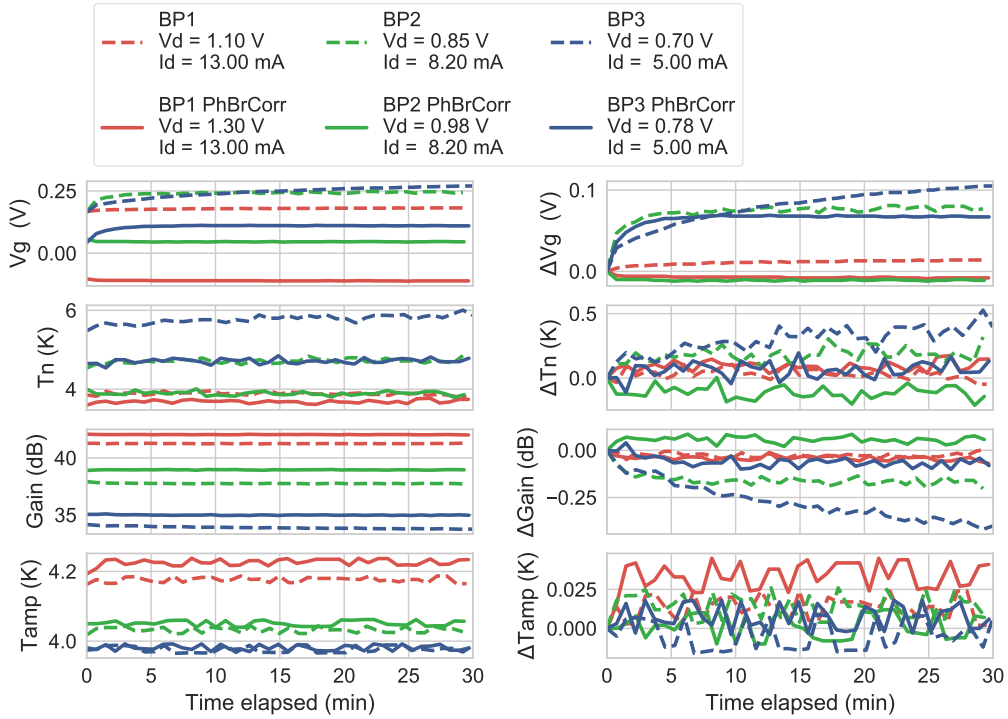


Figure 10: Time series data for amplifier LNF-LNC4\_16NRAOA, s/n 010Z, for three bias points (color), with (solid) and without (dashed) correction for the DC bias wire resistance. Axes on the left show the measured values over time of the gate voltage, the noise temperature and gain at 8 GHz, and the amplifier body physical temperature, from top to bottom. The axes on the right show the difference from the initial values, to more clearly show how they change over time.

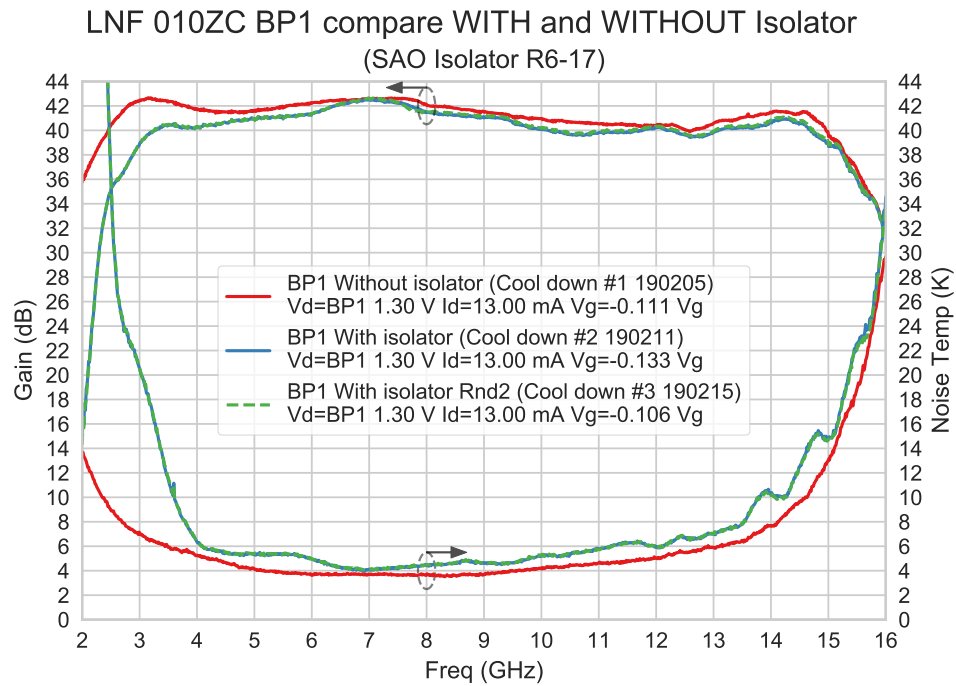


Figure 11: Comparison of the noise temperature and gain for amplifier LNF-LNC4.16NRAOA, s/n 010Z, with (blue and green) and without (red) the SAO isolator at the input. The highest power dissipation bias setting, BP1, was used with values indicated in the legend. The amplifier with the isolator was measured during two separate thermal cycles of the test system, with the dates indicated in the legend (format YYMMDD). These two data are nearly coincident with each other.

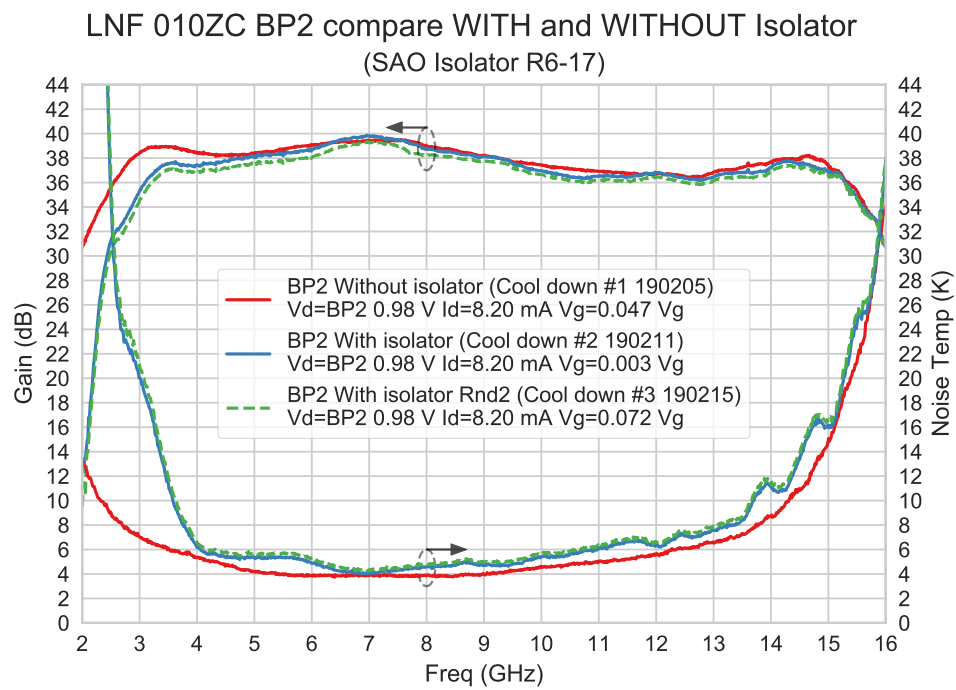


Figure 12: Similar to figure 11, for medium power dissipation bias. Note that with lower power, there is a larger discrepancy between thermal cycles for the results with the isolator.



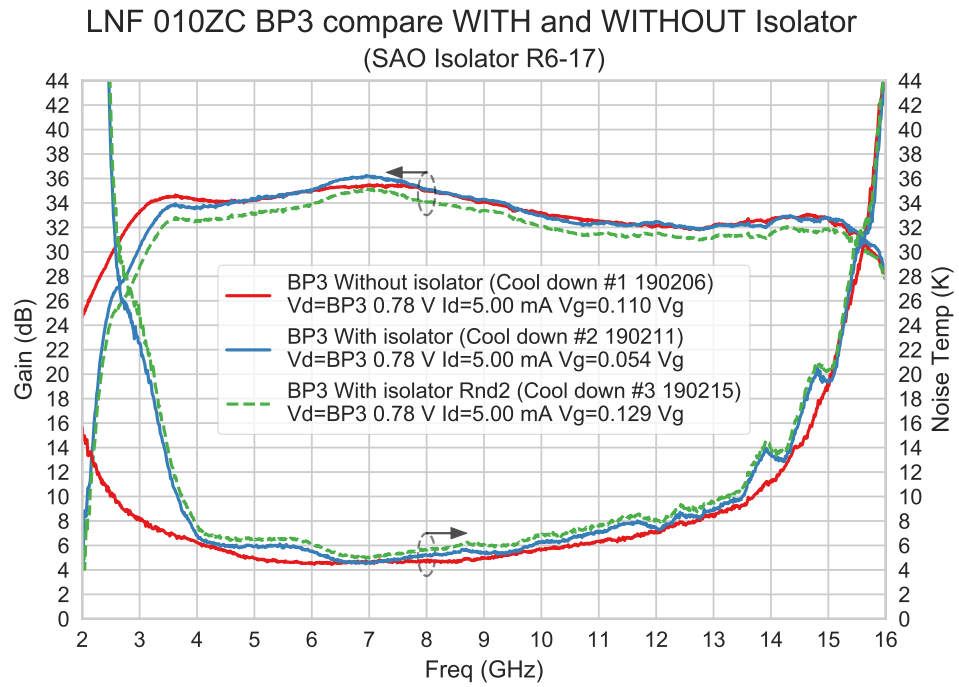


Figure 13: Similar to figures 11 and 12, for lowest power dissipation bias. The discrepancy between thermal cycles for results with the isolator are even more pronounced as compared to the results in figure 12.